Single Carbon Nanotube-Based Reversible Regulation of Biological Motor Activity

Yuichi Inoue,[†] Mitsunori Nagata,[†] Hiroshi Matsutaka,[†] Takeru Okada,[‡] Masaaki K. Sato,[†] and Akihiko Ishijima*,[†]

[†]Institute of Multidisciplinary Research for Advanced Materials, Tohoku University, Aoba-ku, Sendai, 980-8577, Japan and [‡]Institute of Fluid Science, Tohoku University, Aoba-ku, Sendai, 980-8577, Japan

ABSTRACT Because of their small size and high thermal conductivity, carbon nanotubes (CNTs) are excellent candidates for exploring heat transfer at the level of individual molecules in biological research. With a view toward examining the thermal regulation of single biomolecules, we here developed single CNTs as a new platform for observing the motile activity of myosin motors. On multiwall CNTs (diameter ~170 nm; length ~10 μm) coated with skeletal-muscle myosin, the ATP-driven sliding of single actin filaments was clearly observable. The normal sliding speed was ~6 μm/s. Locally irradiating one end of the CNT with a red laser (642 nm), without directly irradiating the active myosin motors, accelerated the sliding speed to ~12 μm/s, indicating the reversible activation of protein function on a single CNT in real time. The temperature along the CNT, which was estimated from the temperature-dependence of the sliding speed, decreased with the distance from the irradiated spot. Using these results with the finite element method, we calculated a first estimation of the thermal conductivity of multiwall CNTs in solution, as 1540 ± 260 ($Wm^{-1} K^{-1}$), which is consistent with the value estimated from the width dependency of multiwall CNTs and the length dependency of single-wall CNTs in a vacuum or air. The temporal regulation of local temperature through individual CNTs should be broadly applicable to the selective activation of various biomolecules *in vitro* and *in vivo*.

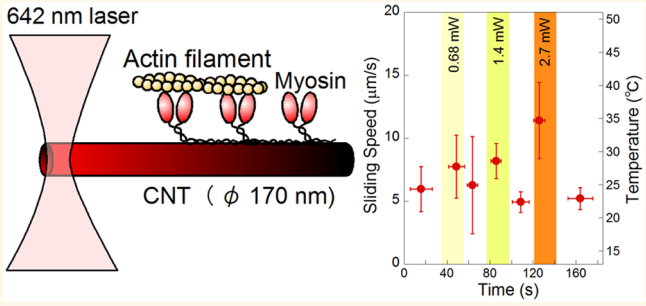

KEYWORDS: molecular motor · myosin · carbon nanotube · laser-induced heating · thermal conductivity

The unique physical and electrical properties of carbon nanotubes (CNTs), including their mechanical strength, electrical conductivity, and optical properties, may prove valuable in several fields of biological research, including drug delivery systems, tissue scaffold reinforcements, and cellular sensors.[1] CNTs have an unusually high thermal conductivity—higher than that reported for any other material, including metals such as gold and copper (320 and 398 $Wm^{-1} K^{-1}$ at room temperature, respectively). The thermal conductivity of single-wall CNTs at room temperature is reported to be 6600 $Wm^{-1} K^{-1}$ by molecular dynamic simulations,[2] and 3500 $Wm^{-1} K^{-1}$ by experimental measurement.[3] The thermal conductivity of multiwall CNTs has been measured to be 2000−3000 $Wm^{-1} K^{-1}$.[4,5] Since their thermal conductivities are much higher than those of metals, CNTs are an excellent candidate material for exploring heat transfer at the level of individual protein molecules.

For biological applications, CNTs must be dispersed as individual tubes in solution and must be functionalized by the adsorption of biomolecules without the loss of biomolecular activities. Since raw CNTs have an affinity for each other, they have usually been dispersed by covalent functionalization[6] or by the use of organic or biological materials, polymers, or surfactants in a solvent.[7] Recently, single protein molecules were successfully adsorbed onto a single CNT, and the enzymatic behavior of proteins such as DNA polymerase I,[8] cAMP-dependent protein kinase A,[9] and lysozyme[10] was assessed by measuring electrical signals through the CNT.

In the 600−1100 nm wavelength range of near-infrared (NIR) light, the NIR light is relatively harmless to biological tissue due to its minimal absorption by hemoglobin

* Address correspondence to ishijima@tagen.tohoku.ac.jp.

Received for review October 2, 2014 and accepted March 13, 2015.

Published online March 13, 2015
10.1021/nn505607c

(<650 nm) and water (>900 nm).[11] CNTs can effectively absorb NIR; thus, NIR laser irradiation (1064 nm wavelength, 1536 mW power) can induce a local rise in temperature in mammalian tissue, to as high as 172 °C.[12] The photothermal effect of continuous NIR irradiation (808 nm wavelength, 50−500 mW power) on single-wall CNTs effectively ablates cancer cells such as HeLa cells[13] and human lung cancer NCI-H460 cells.[14] Notably, the intermittent laser irradiation (1064 nm wavelength, 1 W power) of multiwall CNT-labeled cancer cells kills the cancer cells by increasing their temperature to ~90 °C without harming healthy cells in the surrounding tissue,[15] suggesting that heated CNTs can be used to regulate biomolecular activity. The local irradiation of a single CNT with NIR light would only heat individual biomolecules that are directly adsorbed onto the CNT. This method may serve as a new tool for regulating the activity of single biomolecules.

Skeletal-muscle myosin is a biological motor that converts the free energy of ATP hydrolysis into mechanical work to drive muscle contraction with interacting actin filaments.[16] Fluorescently labeled actin filaments are observed under fluorescence microscopy,[17] and the sliding movement of single actin filaments propelled by glass-adsorbed myosin molecules is directly visualized in the presence of ATP.[18] The observation of ATP-driven sliding, which is distinct from the Brownian movement and passive flow of the solution, provides evidence that active myosin molecules are present on the substrate used in the experiment. This *in vitro* motility assay has been used to examine the chemomechanical cycles of molecular motors such as myosin and kinesin,[19] and more recently, to develop artificial nanotransportation systems.[20]

Recently, CNTs have been combined with molecular motors to transport CNT by myosin[21] and for the motor-powered translocation of biomolecules along tracks of CNTs or semiconductor nanowires.[22,23] Therefore, molecular motors may prove useful for testing CNTs as novel nanoheaters that regulate the activity of individual biomolecules. These molecular motors have typical protein functions, such as molecular recognition, the polymerization of components, and enzymatic activity, as well as energy transduction.

We previously analyzed the chemomechanical cycle of skeletal myosin using *in vitro* motility assays[24] and the temperature dependence of myosin motility using rapid temperature control to measure single molecules.[25] In this study, we developed single CNTs coated with myosin molecules as a track on which to observe the sliding of single actin filaments under fluorescence microscopy. By locally irradiating one end of the CNT during actin filament sliding, we demonstrated that a single CNT can function as a heat conductor to regulate protein activity in real time.

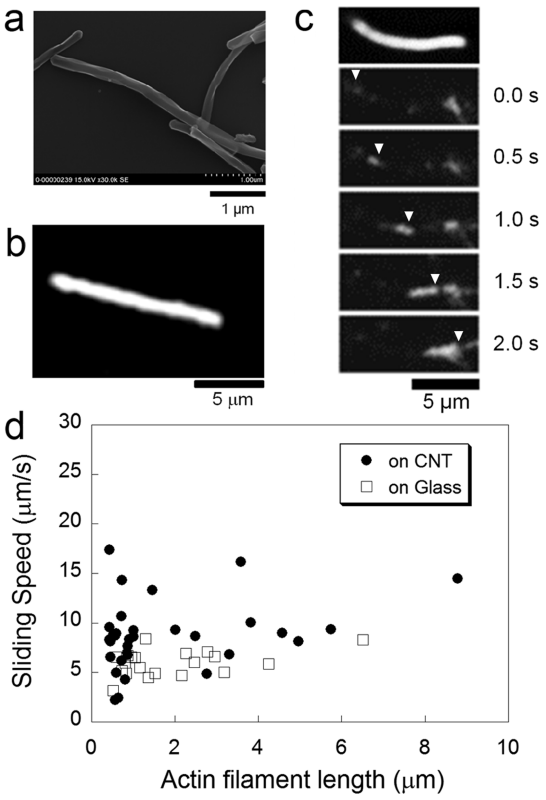

Figure 1. Sliding movement of single actin filaments along a myosin-coated CNT. (a) SEM image of a 170 nm CNT in a vacuum. (b) Dark-field image of a 170 nm CNT in water. (c) Dark-field image of a myosin-coated CNT (top). Fluorescence images of a fluorescently labeled actin filament moving along a CNT (second−bottom). Arrows indicate the leading edge of the actin filament shown in sequential images. (d) The sliding speed of actin filament, plotted against the length of the filament. Filled circles show speeds measured on the myosin-coated CNT (8.7 ± 3.5 μm/s); open squares show speeds on a myosin-coated glass surface without a CNT (6.0 ± 1.2 μm/s). These experiments used a monomeric form of myosin motors at a room temperature of 33 °C.

RESULTS

Actin Filament Sliding along a Myosin-Coated CNT. Figure 1a,b shows images of the multiwall CNTs that were mainly used in this study. The mean CNT diameter measured from images obtained with a scanning electron microscope (Figure 1a) was 174 ± 51 nm ($n = 61$), and the mean CNT length measured from dark-field images in water (Figure 1b) was 8.3 ± 4.2 μm ($n = 51$). The CNTs were coated with myosin molecules and fixed to a glass surface. A myosin-coated CNT, which exists as a single fiber, was selected by the scattered light intensity of the dark-field image (Figure 1c, top, Figure S1, Supporting Information). Then, fluorescently labeled actin filaments were applied to the CNTs and were observed under fluorescence microscopy in the presence of ATP (Figure 1c) to visualize the sliding of a short actin filament along the myosin-coated CNT. Figure 1d shows the sliding speed and length of an actin filament, measured on a myosin-coated CNT (circles). The results were compared with results from conventional *in vitro* motility assays, in which

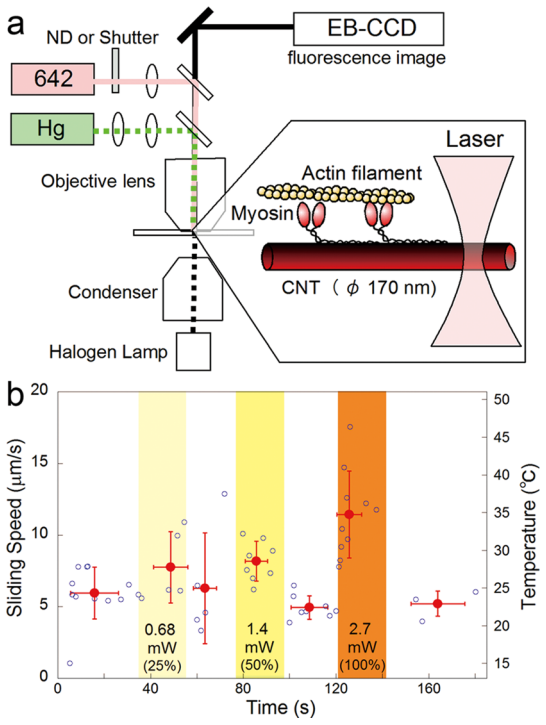

Figure 2. Laser-induced activation of actomyosin sliding speed on single CNTs. (a) Schematic of the experimental system. An optical microscope, used for both dark-field and fluorescence imaging, was combined with a 642 nm laser, which was used to locally irradiate one end of a CNT. A shutter or a neutral density filter was used to induce controlled temporal changes in laser irradiation while observing the movement of actin filaments sliding along a myosin-coated CNT. (b) The sliding speed of actin filament in response to laser irradiation. Blue circles show the speed of individual actin filaments that moved along and detached from the myosin-coated CNT. Red circles show averaged speeds with standard deviations. The average speed increased with increasing laser power (from 0 to 0.68, 1.4, and 2.7 mW) in a reversible fashion. Experiments were performed using myosin filaments at a room temperature of 20 °C.

myosin molecules were directly adsorbed onto a glass surface (squares). The speed of sliding on the myosin-coated glass surface changed little, if at all, with the length of the actin filament.[26] Similarly, the speed on the myosin-coated CNT did not change significantly with the length of the actin filament, and the length and average speed (8.7 ± 3.5 μm/s, n = 32) were comparable to those on the glass surface (6.0 ± 1.2 μm/s, n = 20), suggesting that myosin motors adsorbed onto a CNT retain their normal motile activity.

Activation of Sliding Speed by the Laser Irradiation of Single CNTs. Figure 2a shows the experimental system for locally activating myosin motors. An optical microscope used for the dark-field imaging of CNTs and for the fluorescence imaging of actin filaments was combined with a laser (642 nm) for the local irradiation of a CNT. The laser beam diameter was set to ~2 μm at the sample plane, and the laser power was set to not exceed 2.7 mW (unless otherwise noted), so that both the radiation pressure on the CNT and the convection

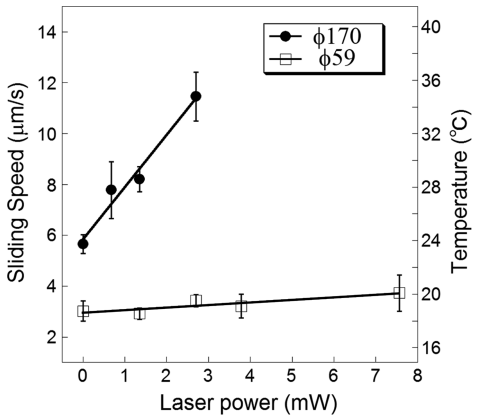

Figure 3. Relationship between sliding speed and laser power on single CNTs. The averaged speeds in Figure 2 were plotted against laser power for the 170 nm CNT (circles) and 59 nm CNT (squares). The slopes of the fit lines were 2.05 and 0.10 μm s^{-1} mW^{-1} for the 170 nm CNT and the 59 nm CNT, respectively. Error bars are standard error of the mean. Numbers of actin filaments for the 170 nm CNT were 29, 5, 8, and 10, and for the 59 nm CNT were 56, 18, 23, 5, and 6. The experiments were performed using myosin filaments at a room temperature of 20 °C.

of the solution around the CNT were negligible. One end of the CNT was irradiated for ~20 s with the laser, and the sliding speed of each actin filament that moved along and dissociated from the myosin-coated CNT was measured (Figure 2b, blue circles). The speed prior to laser irradiation, 6.0 ± 1.8 μm/s on average at a room temperature of 20 °C, increased slightly to 7.8 ± 2.5 μm/s with 0.68 mW irradiation, and returned to 6.3 ± 3.9 μm/s when the irradiation was paused. The drop in speed when the irradiation was paused suggests that the temperature rise of the entire solution during the 20 s of irradiation was negligible. The sliding speed was repeatedly accelerated to 8.2 ± 1.4 and 11.4 ± 3.0 μm/s by 1.4 and 2.7 mW irradiation, respectively.

Temperature on 170 and 59 nm CNTs. The activation assay was performed using both the 170 nm diameter CNT and a thinner CNT with a diameter of 58.6 ± 13.2 nm (n = 91). Figure 3 shows the sliding speeds according to irradiation power; the right axis shows the conversion of speed to the temperature of the myosin using the linear relationship between sliding speed and temperature in the range of 16−40 °C (Figure S2), which was determined in our previous study.[25] The sliding speed increased linearly with increasing laser irradiation of the 170 nm CNT to 2.7 mW, as shown in Figure 2. This speed increase corresponded to a temperature jump of ~12 °C for myosin. However, laser irradiation barely increased the sliding speed on the 59 nm CNT; even at 7.6 mW, the rise in temperature induced on the 59 nm CNT was as little as ~1.5 °C.

Temporal Speed Changes of Single Actin Filaments. To show the laser-induced regulation of myosin motors more clearly than by the average speed change shown in Figure 2, we observed the temporal speed changes of single actin filaments while applying intermittent

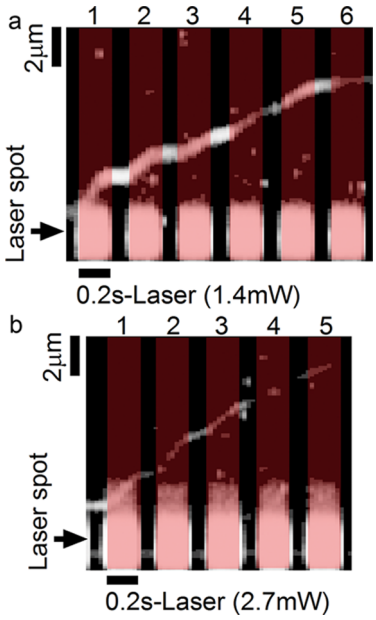

Figure 4. Repetitive activation of single actin filament during sliding. (a) Kymograph showing the position of a single actin filament in the longitudinal direction and time in the transverse direction. The sliding movement was accelerated repeatedly by repeating the 1.4 mW laser irradiation of ~0.2-s duration. (b) Kymograph generated with a 2.8 mW laser. The experiments were performed using myosin filaments at a room temperature of 20 °C.

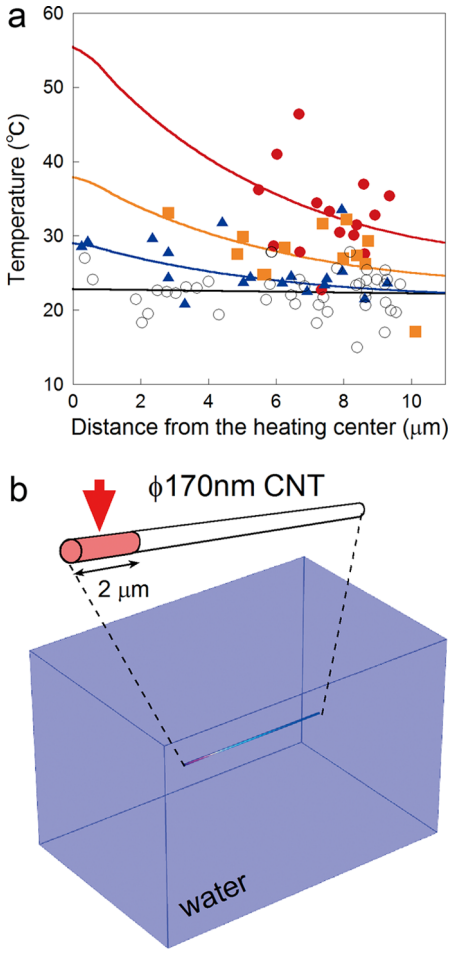

Figure 5. Temperature distribution along the 170 nm CNT. (a) The calculated temperatures were plotted against the distance from the laser-irradiated spot. Speeds measured during the 20-s laser irradiation (Figure 2) were converted to the temperature of the myosin motors, as described in the main text. Distance was measured from the center of the irradiated spot to the midpoint of the sliding observed on the CNT. The laser powers used were 0 mW (open circles), 0.68 mW (blue triangles), 1.4 mW (orange squares), and 2.7 mW (filled red circles). Fitted lines were derived by calculations using the FEM model shown in b. (b) A 3D model for the finite element method. A 170 nm CNT is surrounded by a large amount of water (a cuboid of 20 × 20 × 30 μm^3). The heat conduction from an end point of the CNT (2-μm length, as a heat source) into the rest of the CNT (15 μm in length and 170 nm in diameter), and the surrounding water was numerically solved (see text) using a boundary condition of constant temperature (20 °C) at the 6 planes of the water cuboid.

laser irradiation. Figure 4 is a kymograph showing the time course of the position of a short actin filament in response to laser irradiation for 0.2 s (highlighted by pink bars) of the 170 nm CNT. The sliding speed was strongly accelerated by laser irradiation, indicating that the myosin motor could be rapidly regulated (<1 s response time). The laser-induced acceleration of the single actin filament in Figure 4, which moved from the vicinity of the irradiation spot to the end of the CNT, was clearly evident in the first and second irradiation, but was more moderate in the third to sixth irradiation periods, suggesting that the acceleration may depend on the distance from the irradiated spot. We used the temperature profile along the single CNT to calculate the thermal conductivity of the 170 nm CNT (see Discussion) (Figure 5).

DISCUSSION

Observation of Protein Function on a Single CNT. In this study, we clearly demonstrated the sliding of a single actin filament along a single myosin-coated CNT (Figure 1), with a sliding speed comparable to that reported for a glass surface.[26] For *in vitro* motility assays on a glass surface, the threshold density of myosin molecules required for the sliding of 1.1-μm-long actin filaments is reported to be 600 μm^{-2}.[27] Using the band model[28] with a bandwidth of ~30 nm (determined from electron micrographs of the actin-myosin complex),[29] the threshold number of myosin motor domains required for sliding is calculated to be 19.8. In the present study using CNTs and actin filaments with an average length of 1.80 ± 0.35 μm (mean ± SEM, n = 32), the minimum myosin density on the CNTs needed to observe sliding was estimated to be 367 μm^{-2}.

Recently, CNT-based measurements of protein activities were reported for DNA polymerase I,[8] cAMP-dependent protein kinase A,[9] and lysosome,[10] as well as the motor proteins kinesin[22] and myosin.[23] However, the measured activity does not always reflect the physiological activity of the proteins. For example, the sliding speed of kinesin on a bundle of several CNTs is

lower than its physiological speed (<20% of the speed obtained on a glass surface),[22] as is that of myosin on semiconductor nanowires (~42% of the speed on a glass surface).[23] The lower sliding speed might be due to damage to the motors on the substrates. Such damage can be prevented by precoating the surface with nitrocellulose[28] or "Sigmacote".[26] In the present study, Tween20 was used to precoat the CNT surface, and myosin filaments, in which the exposed myosin remains active even when myosin motor domains in the CNT-filament interface are damaged, were used in most of the experiments.

The normal level of myosin motility on the CNT demonstrated in this study shows that a single CNT can be used as a platform to examine the normal functions of proteins, including myosin motors. Furthermore, the sliding speed was temporally activated by the local laser irradiation of one end of the CNT (Figures 2–4), indicating that myosin molecules were irreversibly attached to the CNTs to drive the sliding of actin filaments. Our results suggest that multiwall CNTs may be a powerful platform for regulating the authentic functions of motor proteins by external heat in real time, as well as for measuring their activities.

Temperature Rise Induced by Laser Irradiation. It has been reported that rapid temperature changes can be induced in motor proteins by 1053 nm laser irradiation (50–100 mW) on a 2-dimensional metal surface.[30,31] We found that a 2-dimensional heat conductor could be achieved using a planar aggregate of 170 nm CNTs (Figure S3), and that a single 170 nm CNT could induce a temperature increase in myosin molecules of ~12 °C (Figures 2 and 3) through local laser irradiation, suggesting that a single 170 nm CNT could efficiently convert NIR light into heat. When the laser power applied to a 170 nm CNT was increased to 4 mW or more, the sliding speed was irreversibly reduced, due to the thermal denaturation of myosin molecules over 40 °C (Figure S4). Raising the laser power to more than 30 mW caused bubbles to be generated at the irradiation point on the 170 nm CNT, possibly by the evaporation of water as well as the convective flow of the solution. Therefore, the temperature induced by irradiating a single 170 nm CNT could be increased to 100 °C or more, as reported for the heating of mammalian tissue using multiple multiwall CNTs.[12]

On the other hand, laser irradiation of the end of the 59 nm CNT resulted in only a small change in the actin-filament sliding speed and temperature (Figure 3). The slope for the 59 nm CNT shown in Figure 3 was 0.10 μm s^{-1} mW^{-1}; the slope for the 170 nm CNT was 20-times higher than this. Because temperature dependences of sliding speeds on both CNTs were similar when the room temperature was changed, this ~20-fold difference might be due to differences in the diameter and/or the physical properties of the CNTs. Resonance Raman spectra with similar G/D ratios suggested that the crystallinity of the two types of CNTs is similar (Figure S5). If the 59 and 170 nm CNTs share the same absorption coefficient, the laser-induced heat in the 170 nm CNT is calculated to be ~4.1-fold greater than that of the 59 nm CNT (Supporting Information Discussion), suggesting that the temperature rise on the 170 nm CNT is also ~4-fold greater than that on the 59 nm CNT (Figure S6). The ~20-fold *versus* the ~4-fold difference might be owing to differences in the physical properties between the 59 and 170 nm CNTs, mainly that the 59 nm CNT has a smaller absorption coefficient than the 170 nm CNT (Supporting Information Discussion), possibly due to the lower density of multiwalls in the 59 nm CNT. It is reported that the heat conduction in multiwall CNTs is highly anisotropic, such that the in-shell thermal conductivity (λ_{in} = 1800 Wm^{-1} K^{-1}, along the CNT) is much larger than the out-of-shell thermal conductivity (λ_{out} = 0.05 Wm^{-1} K^{-1}, in cross section).[32] Our results may suggest that the number of multiwalls and the CNT cross-sectional density have important effects on the light-to-heat conversion on the CNT and on the heat conduction that occurs in the cross-sectional direction before heat is transferred along the CNT.

Thermal Conductivity of Multiwall CNTs. To examine the temperature distribution along the 170 nm CNT, the temperature estimated from the speed of each actin filament in Figure 2b was plotted along with each filament's position on the CNT (Figure 5a). The temperatures estimated for the 0.68, 1.4, and 2.7 mW laser irradiations declined as the distance from the irradiated spot increased. The heat transfer from the irradiated spot was calculated by the finite element method (FEM) using a 3-dimensional model of a CNT surrounded by a large amount of water (Figure 5b). Heat conduction from the irradiated spot into the rest of the CNT and to the surrounding water was numerically solved using the boundary conditions described in the figure legend. The FEM calculation was repeated with various values for the thermal conductivity of the CNT (k) and the power of the heat source (Q) to find the best fit to the experimental data along a CNT (Figure 5a). The k and Q values that minimized the sum of the squared differences between the experimental data and the calculated value were 1540 ± 260 (Wm^{-1} K^{-1}) and 263 ± 84 (μW), respectively (Figure S7).

The reported thermal conductivity at room temperature, 120–6600 Wm^{-1} K^{-1} for single-wall CNTs and 120–3000 Wm^{-1} K^{-1} for multiwall CNTs, generally depends on such factors as diameter and length.[4,5,33,34] For multiwall CNTs with a length of ~2.5 μm and a diameter of 14, 80, or 200 nm, the thermal conductivities were measured to be ~3000, ~2000, and ~400 Wm^{-1} K^{-1}, respectively.[4] On the basis of these results, the thermal conductivity of our 170 nm CNT was estimated to be ~800 Wm^{-1} K^{-1} for

lengths as short as ~2.5 μm. Molecular dynamics simulation for the single-wall CNT suggested that thermal conductivity increases as the length of the CNT increases.[34,35] If the length-dependency of the single-wall CNT at 316 K[35] is true for the multiwall CNT at ~300 K, a ~6-fold increase in CNT length—from 2.5 to 15 μm—would induce a ~2.2-fold increase in the thermal conductivity of the 170 nm CNT, from ~800 to ~1760 Wm^{-1} K^{-1} (calculated from the previous results[4,35]). This result is consistent with our estimation of 1540 $\pm$ 260 Wm^{-1} K^{-1}. Therefore, the high thermal conductivity of the 170 nm CNT will ensure that the CNT functions as a heat conductor for various biomolecules, including motor proteins. The thermal conductivity of CNTs has been reported by molecular dynamics simulations and experiments in a vacuum or air. To the best of our knowledge, this is the first report estimating the thermal conductivity of CNTs in an aqueous solution. It is also the first to calculate this thermal conductivity using a biomolecular function. Our estimation of 1540 $\pm$ 260 Wm^{-1} K^{-1} is similar to the in-shell thermal conductivity (λ_{in} = 1800 Wm^{-1} K^{-1}, along the CNT) determined from the model of a comparably sized multiwall CNT (outer diameter ~90 nm and length ~5 μm) and the experimental result in a vacuum of 400 Wm^{-1} K^{-1} or less.[32] Therefore, our system may be useful for understanding the anisotropic heat conduction in multiwall CNTs.

CONCLUSION

The photothermal effect of CNTs under NIR irradiation has been used to ablate cancer cells[13,14] by heating and by generating reactive oxygen.[14] In contrast to the ablation experiments on cancer cells, which use a huge number of CNTs, a distinctive feature of this study is that the regulation of biomolecules was locally targeted to a single CNT. The ability to locally target intracellular organelles and/or proteins using CNTs is important for controlling events at the subcellular or single-molecular level. Another important feature of this study is that the biomolecules were regulated in a reversible mode over a temperature range of 20−40 °C; in these experiments, reactive oxygen was removed by enzymatic reactions for continuous fluorescence imaging,[26] and pH changes were minimized by using a buffer. However, the reversible mode could easily change to an irreversible one by extensive heating over 40 °C (Figure S4), which inactivates most proteins irreversibly through thermal denaturation. The flexible control of protein function and local targeting on a single CNT, demonstrated in this study, should be useful for future applications of CNTs in biophysics and biomedicine.

METHODS

Chemicals and Proteins. Unless otherwise noted, chemicals were obtained from Wako (Wako Pure Chemical Industries, Ltd. Japan). Skeletal myosin and actin filaments were extracted from rabbit skeletal muscle and purified as described previously.[26] The 170 nm diameter multiwall carbon nanotubes were obtained from Materials Technologies Research (MTR Ltd., Cleveland, OH, USA). The 59 nm diameter multiwall carbon nanotubes were provided by Tsukuba Materials Information Laboratory (TMIL, Ltd., Japan). Images of the CNTs in a vacuum were obtained with a scanning electron microscope (SU6000, Hitachi, Japan). All experimental procedures and rabbit care followed the regulations for animal experiments and related activities at Tohoku University.

Myosin-Coated CNTs. To improve CNT dispersion, CNTs (1 mg) were mixed with 1.5 mL of 25 mM buffer [25 mM KCl, 20 mM HEPES-KOH (pH 7.0), and 5 mM $MgCl_2$] and combined with 0.5 mL of Tween20 solution (40350−02, Kanto Kagaku Co., Inc., Japan) for 10 h at room temperature. The solution was centrifuged for 3 cycles (21500*g*, 20 min), the precipitate was lysed (2 mL), and the CNT solution was washed to remove unbound Tween20 (Tween-CNT). Skeletal myosin (~30 mg/mL) was diluted with 25 mM buffer to 1.0 mg/mL to form myosin filaments. Myosin filaments were adsorbed onto the Tween-CNTs by mixing 0.1 mL of myosin solution (1.0 mg/mL) with 0.1 mL of Tween-CNT (1.0 mg/mL) for 30 min at 4 °C. A solution of CNTs coated with myosin filaments (MF-CNT) was prepared by 4 cycles of centrifugation (21500*g*, 1 min, 4 °C) to remove unbound myosin molecules. A solution of CNTs coated with isolated myosin molecules (M-CNT) was prepared similarly using 0.6 M buffer [0.6 M KCl, 10 mM HEPES-KOH (pH 7.0)].

***In Vitro* Motility Assay on CNTs.** MF-CNT (or M-CNT) solution (10 μL) was applied to a slide glass (26 mm × 76 mm; Matsunami, Japan) and sealed with a cover glass (18 mm × 18 mm, Matsunami) on which two corners were bent to form a sample chamber of ~5 μL. After a 2 min incubation to allow the nonspecific binding of MF-CNTs (or M-CNTs), 20 μL of actin solution (0.1 μg/mL, actin filaments stabilized by tetramethylrhodamine-labeled phalloidin[17]) was perfused with an oxygen scavenging system[26] and 2 mM ATP. The chamber was mounted on a microscope (BX51, Olympus, Japan) with an oil immersion lens (UPlanApo, 100×, N.A. = 0.5−1.35, Oil; Olympus, Japan). Dark-field images of CNTs and fluorescence images of actin filament were monitored using a camera (EB-CCD, C7190, Hamamatsu, Japan); images were recorded at 30 frames/s with a personal computer using a video-to-USB converter (DFG/USB2pro; The Imaging Source Europe GmbH, Bremen, Germany).

Laser Irradiation of a Single CNT. A 642 nm laser (Excelsior-642C-60-CORH, Spectra-Physics, USA) was introduced to the BX51 microscope so that a laser beam was focused ($\phi \sim 2$ μm) on the sample plane to heat a single CNT locally at one end. The power of the laser irradiation was reduced to 0.68−2.7 mW at the nosepiece of the objective lens by replacing neutral density filters. The timing of the laser irradiation was controlled by manipulating an electronic shutter (F573 and F116, Suruga Seiki Co., Ltd., Japan) using an AD converter (NI USB-6008, National Instruments, Austin, TX, USA) with programs written in LabVIEW 2009 (National Instruments, Austin, TX, USA).

Calculation of Speed and Temperature. Video images were analyzed using ImageJ software (NIH, USA) and LabVIEW 2009 software. The sliding speed was calculated from the travel distance of an actin filament for more than 4 video frames. The sliding speed was converted to the temperature of the myosin motors by the temperature-dependence of speed, as described in the main text. The 3-dimensional distribution of temperature around a CNT was derived from the equation of heat conduction by the FEM using COMSOL Multiphysics (COMSOL AB, Stockholm, Sweden) as described in the Discussion. In general, a rise in temperature accelerates all chemical reactions, including the enzymatic activity of proteins. At low temperatures (≪ 20 °C), the slow ATPase activity of a motor protein produces only a small amount of displacement, which is difficult to detect by video analysis. On the other hand, at high

temperatures (>40 °C), most proteins undergo denaturation, and enzymes irreversibly lose their activity. Therefore, we controlled the temperature at 20−40 °C in this study.

Conflict of Interest: The authors declare no competing financial interest.

Acknowledgment. We thank the Tsukuba Materials Information Laboratory (TMIL, Ltd., Tsukuba, Japan) for providing the 59 nm CNTs, and Prof. F. Arai (Nagoya University, Nagoya, Japan) and Prof. T. Ono (Tohoku University, Sendai, Japan) for discussion. This research was supported by CREST from JST (A.I.); KAKENHI on Innovative Areas from MEXT/JSPS (A.I.); KAKENHI from MEXT/JSPS (A.I., and Y.I.); and the FIRST program from JSPS (A.I. and Y.I.). This research was also supported in part by the Management Expenses Grants for National Universities Corporations from MEXT.

Supporting Information Available: Dark-field images of myosin-coated CNTs (Figure S1); Relationship between sliding speed and temperature (Figure S2); Activation of myosin motors on a planar aggregate of 170 nm CNTs (Figure S3); Relationship between a rise in temperature and the power of the laser irradiation applied to the 170 nm CNT (Figure S4); Resonance Raman spectra measured for the 170 nm and the 59 nm CNTs (Figure S5); The temperature rise calculated by FEM for the 170 nm and the 59 nm CNTs (Figure S6); The thermal conductivity value that minimizes the error with the experimental results (Figure S7); Additional examples of the sliding actin filaments on single myosin-coated CNTs (Figure S8); The sliding movement of a single actin filament along a 59 nm CNT (Figure S9). Movies of sliding actin filament on the myosin-coated CNT without or with laser irradiation (Movies S1 and S2). Movie of sliding actin filaments on a planar aggregate of CNTs (Movie S3). Movie of sliding actin filament on the myosin-coated CNT with continuous laser irradiation, in which the irradiation spot was on the glass surface or on the CNTs (Movie S4). This material is available free of charge *via* the Internet at http://pubs.acs.org.

REFERENCES AND NOTES

1. Cha, C.; Shin, S. R.; Annabi, N.; Dokmeci, M. R.; Khademhosseini, A. Carbon-Based Nanomaterials: Multifunctional Materials for Biomedical Engineering. *ACS Nano* **2013**, *7*, 2891–2897.
2. Berber, S.; Kwon, Y. K.; Tomanek, D. Unusually High Thermal Conductivity of Carbon Nanotubes. *Phys. Rev. Lett.* **2000**, *84*, 4613–4616.
3. Pop, E.; Mann, D.; Wang, Q.; Goodson, K.; Dai, H. Thermal Conductance of an Individual Single-Wall Carbon Nanotube above Room Temperature. *Nano Lett.* **2006**, *6*, 96–100.
4. Kim, P.; Shi, L.; Majumdar, A.; McEuen, P. L. Thermal Transport Measurements of Individual Multiwalled Nanotubes. *Phys. Rev. Lett.* **2001**, *87*, 215502.
5. Fujii, M.; Zhang, X.; Xie, H.; Ago, H.; Takahashi, K.; Ikuta, T.; Abe, H.; Shimizu, T. Measuring the Thermal Conductivity of a Single Carbon Nanotube. *Phys. Rev. Lett.* **2005**, *95*, 065502.
6. Star, A.; Stoddart, J. F. Dispersion and Solubilization of Single-Walled Carbon Nanotubes with a Hyperbranched Polymer. *Macromolecules* **2002**, *35*, 7516–7520.
7. Star, A.; Liu, Y.; Grant, K.; Ridvan, L.; Stoddart, J. F.; Steuerman, D. W.; Diehl, M. R.; Boukai, A.; Heath, J. R. Noncovalent Side-Wall Functionalization of Single-Walled Carbon Nanotubes. *Macromolecules* **2003**, *36*, 553–560.
8. Olsen, T. J.; Choi, Y.; Sims, P. C.; Gul, O. T.; Corso, B. L.; Dong, C.; Brown, W. A.; Collins, P. G.; Weiss, G. A. Electronic Measurements of Single-Molecule Processing by DNA Polymerase I (Klenow Fragment). *J. Am. Chem. Soc.* **2013**, *135*, 7855–7860.
9. Sims, P. C.; Moody, I. S.; Choi, Y.; Dong, C.; Iftikhar, M.; Corso, B. L.; Gul, O. T.; Collins, P. G.; Weiss, G. A. Electronic Measurements of Single-Molecule Catalysis by cAMP-Dependent Protein Kinase A. *J. Am. Chem. Soc.* **2013**, *135*, 7861–7868.
10. Choi, Y.; Olsen, T. J.; Sims, P. C.; Moody, I. S.; Corso, B. L.; Dang, M. N.; Weiss, G. A.; Collins, P. G. Dissecting Single-Molecule Signal Transduction in Carbon Nanotube Circuits with Protein Engineering. *Nano Lett.* **2013**, *13*, 625–631.
11. Weissleder, R. A Clearer Vision for *In Vivo* Imaging. *Nat. Biotechnol.* **2001**, *19*, 316–317.
12. Picou, L.; McMann, C.; Elzer, P. H.; Enright, F. M.; Biris, A. S.; Boldor, D. Spatio-Temporal Thermal Kinetics of *In Situ* MWCNT Heating in Biological Tissues under NIR Laser Irradiation. *Nanotechnology* **2010**, *21*, 435101.
13. Kam, N. W.; O'Connell, M.; Wisdom, J. A.; Dai, H. Carbon Nanotubes as Multifunctional Biological Transporters and Near-Infrared Agents for Selective Cancer Cell Destruction. *Proc. Natl. Acad. Sci. U. S. A.* **2005**, *102*, 11600–11605.
14. Murakami, T.; Nakatsuji, H.; Inada, M.; Matoba, Y.; Umeyama, T.; Tsujimoto, M.; Isoda, S.; Hashida, M.; Imahori, H. Photodynamic and Photothermal Effects of Semiconducting and Metallic-Enriched Single-Walled Carbon Nanotubes. *J. Am. Chem. Soc.* **2012**, *134*, 17862–17865.
15. Biris, A.; Boldor, D.; Palmer, J.; Monroe, W. T.; Mahmood, M.; Dervishi, E.; Xu, Y.; Li, Z.; Galanzha, E. I.; Zharov, V. P. Nanophotothermolysis of Multiple Scattered Cancer Cells with Carbon Nanotubes Guided by Time-Resolved Infrared Thermal Imaging. *J. Biomed Opt.* **2009**, *14*, 021007.
16. Huxley, A. F. Mechanics and Models of the Myosin Motor. *Philos. Trans. R. Soc. London, Ser. B* **2000**, *355*, 433–440.
17. Yanagida, T.; Nakase, M.; Nishiyama, K.; Oosawa, F. Direct Observation of Motion of Single F-Actin Filaments in the Presence of Myosin. *Nature* **1984**, *307*, 58–60.
18. Kron, S. J.; Spudich, J. A. Fluorescent Actin Filaments Move on Myosin Fixed to a Glass Surface. *Proc. Natl. Acad. Sci. U. S. A.* **1986**, *83*, 6272–6276.
19. Block, S. M. Kinesin Motor Mechanics: Binding, Stepping, Tracking, Gating, and Limping. *Biophys. J.* **2007**, *92*, 2986–2995.
20. van den Heuvel, M. G.; Dekker, C. Motor Proteins at Work for Nanotechnology. *Science* **2007**, *317*, 333–336.
21. Tsuchiya, Y.; Komori, T.; Hirano, M.; Shiraki, T.; Kakugo, A.; Ide, T.; Gong, J. P.; Yamada, S.; Yanagida, T.; Shinkai, S. A Polysaccharide-Based Container Transportation System Powered by Molecular Motors. *Angew. Chem., Int. Ed. Engl.* **2010**, *49*, 724–727.
22. Sikora, A.; Ramón-Azcón, J.; Kim, K.; Reaves, K.; Nakazawa, H.; Umetsu, M.; Kumagai, I.; Adschiri, T.; Shiku, H.; Matsue, T.; Hwang, W.; Teizer, W. Molecular Motor-Powered Shuttles along Multi-Walled Carbon Nanotube Tracks. *Nano Lett.* **2014**, *14*, 876–881.
23. Siethoff, L. T.; Lard, M.; Generosi, J.; Andersson, H. S.; Linke, H.; Månsson, A. Molecular Motor Propelled Filaments Reveal Light-Guiding in Nanowire Arrays for Enhanced Biosensing. *Nano Lett.* **2014**, *14*, 737–742.
24. Sato, M. K.; Ishihara, T.; Tanaka, H.; Ishijima, A.; Inoue, Y. Velocity-Dependent Actomyosin ATPase Cycle Revealed by *In Vitro* Motility Assay with Kinetic Analysis. *Biophys. J.* **2012**, *103*, 711–718.
25. Baker, M. A.; Inoue, Y.; Takeda, K.; Ishijima, A.; Berry, R. M. Two Methods of Temperature Control for Single-Molecule Measurements. *Eur. Biophys J.* **2011**, *40*, 651–660.
26. Harada, Y.; Sakurada, K.; Aoki, T.; Thomas, D. D.; Yanagida, T. Mechanochemical Coupling in Actomyosin Energy Transduction Studied by *In Vitro* Movement Assay. *J. Mol. Biol.* **1990**, *216*, 49–68.
27. Toyoshima, Y. Y.; Kron, S. J.; Spudich, J. A. The Myosin Step Size: Measurement of the Unit Displacement per ATP Hydrolyzed in an *In Vitro* Assay. *Proc. Natl. Acad. Sci. U. S. A.* **1990**, *87*, 7130–7134.
28. Uyeda, T. Q.; Kron, S. J.; Spudich, J. A. Myosin Step Size. Estimation from Slow Sliding Movement of Actin over Low Densities of Heavy Meromyosin. *J. Mol. Biol.* **1990**, *214*, 699–710.
29. Toyoshima, Y. Y.; Toyoshima, C.; Spudich, J. A. Bidirectional Movement of Actin Filaments along Tracks of Myosin Heads. *Nature* **1989**, *341*, 154–156.
30. Kato, H.; Nishizaka, T.; Iga, T.; Kinosita, K., Jr.; Ishiwata, S. Imaging of Thermal Activation of Actomyosin Motors. *Proc. Natl. Acad. Sci. U. S. A.* **1999**, *96*, 9602–9606.

31. Kawaguchi, K.; Ishiwata, S. Thermal Activation of Single Kinesin Molecules with Temperature Pulse Microscopy. *Cell Motil. Cytoskeleton.* **2001**, *49*, 41–47.
32. Hayashi, H.; Ikuta, T.; Nishiyama, T.; Takahashi, K. Enhanced Anisotropic Heat Conduction in Multi-walled Carbon Nanotubes. *J. Appl. Phys.* **2013**, *113*, 014301.
33. Yang, J.; Yang, Y.; Waltermire, S. W.; Gutu, T.; Zinn, A. A.; Xu, T. T.; Chen, Y.; Li, D. Measurement of the Intrinsic Thermal Conductivity of a Multiwalled Carbon Nanotube and its Contact Thermal Resistance with the Substrate. *Small* **2011**, *7*, 2334–2340.
34. Cao, A.; Qu, J. Size Dependent Thermal Conductivity of Single-Walled Carbon Nanotubes. *J. Appl. Phys.* **2012**, *112*, 013503.
35. Mingo, N.; Broido, D. A. Length Dependence of Carbon Nanotube Thermal Conductivity and the Problem of Long Waves. *Nano Lett.* **2005**, *5*, 1221–1225.